

Improved estimates for the fall speed of sub-100 μm ice crystals

C. D. Westbrook

Department of Meteorology, University of Reading, UK.

Abstract: New theoretical results are presented for the sedimentation rate of realistic ice crystals at sizes smaller than 100 μm . The calculations, which exploit a mathematical analogy with electrostatics, are compared with laboratory studies and found to be in good agreement. These results highlight a weakness in contemporary ice particle fall speed parameterisations for very small crystals, which can lead to sedimentation rates being overestimated by a factor of two. The potential of Doppler lidar measurements to determine the radiative importance of these small ice crystals in cirrus clouds is considered as an application. The theoretical framework presented here may also be useful for calculating the sedimentation rate and mobility of non-spherical aerosol particles. Copyright © 2007 Royal Meteorological Society

KEY WORDS class file; $\text{\LaTeX} 2_{\epsilon}$; *Q. J. R. Meteorol. Soc.*

Received 5 January 2007; Revised ; Accepted

1 Introduction

The sedimentation of natural ice particles is fundamental to the evolution of the ice phase in clouds, influencing almost all of the relevant microphysical processes including deposition, riming, aggregation, evaporation and melting. Modelling the sedimentation velocity v of ice crystals is challenging because they are almost universally non-spherical in shape, and span a range of flow regimes. Whereas a rather accurate formula exists for the drag on a sphere (Abraham 1970), theoretical progress for non-spherical particles is more difficult. Importantly, Böhm (1989) and Mitchell (1996) have attempted to modify Abraham's formulation for an ice particle of arbitrary shape: Mitchell argues that the results are likely to be accurate to within $\sim 20\%$ over the whole range of flow regimes experienced by ice particles in the atmosphere. His piecewise fits have recently been refined to provide a continuous power law with variable co-efficients (Khvorostyanov and Curry 2002), and further adjustments have been made for turbulence at high Reynolds number (Mitchell and Heymsfield 2005, Khvorostyanov and Curry 2005). This framework is very appealing because of its generality, but there is a need to test it, particularly at small and large Reynolds numbers where the boundary-layer ideology underpinning it breaks down.

The radiative importance of ice crystals smaller than 60 μm in cirrus clouds remains a controversial issue. Aircraft measurements have indicated that these tiny crystals may exist in very large concentrations (see Heymsfield and McFarquhar 2002) and could dominate the optical properties of the cloud; on the other hand, there is also

evidence to suggest that some of the measurements of this small crystal mode are an artefact of larger crystals shattering on the probe inlet (Field *et al.* 2003, McFarquhar *et al.* 2007). Doppler lidar observations have an opportunity to inform this debate, since if these tiny crystals were to dominate the optical properties of the cloud, they should also dominate the lidar backscatter and Doppler velocity. Given accurate estimates of the sedimentation rates of these small ice crystals, there is an opportunity to compare these values with the measured frequency distribution of lidar Doppler velocities in cirrus clouds, and to determine whether or not sub-60 μm crystals genuinely have a significant impact on the optical properties of cirrus.

The aim of this short paper is to investigate the sedimentation rates of ice crystals at relatively low Reynolds number, focussing on crystals smaller than around 100 μm where viscous forces dominate the flow. The theoretical results are compared to experimental data, and also to the fall-speed parameterisations referred to above (Mitchell 1996, Mitchell and Heymsfield 2005, Khvorostyanov and Curry 2002, 2005 - from now on collectively referred to as MHKC).

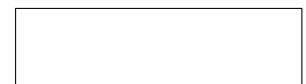
2 Viscous sedimentation speeds

When the Reynolds number $\text{Re} = vD/\nu_k$ is small, viscous forces dominate the flow. Here D is taken to be the maximum span of the crystal (following Heymsfield *et al.* 2002), and ν_k is the kinematic viscosity of air. The Stokes solution for a sphere in a viscous flow is well known:

$$v = \left(\frac{g}{6\pi\eta} \right) \times \frac{m}{R} \quad (1)$$

where m and R are the particle mass and radius respectively, g is the acceleration due to gravity, and η is the

*Correspondence to: Dr. Chris Westbrook, Department of Meteorology, University of Reading, Earley Gate, Reading, Berkshire, RG6 6BB, UK. E-mail: c.d.westbrook@reading.ac.uk



viscosity of the air. Dimensional analysis suggests that an identical formula should exist for non-spherical ice particles falling in a given orientation, but with some ‘effective radius’ in place of the sphere radius. The problem then is to determine this effective radius for natural ice crystals.

A number of theoretical works suggest that the particle length scales characterising viscous drag may be closely related to those characterising electrostatic and molecular diffusion problems. In particular the *capacitance* of the particle (in length units) seems to play an important role (Hubbard and Douglas 1993, Roscoe 1949). This seems sensible since the drag in viscous flow is essentially the product of momentum (or vorticity) diffusing away from the falling crystal. Westbrook *et al.* (2008) have recently calculated the capacitance C of a variety of realistic crystal habits using a random walker sampling method. The data from that work is applied below to assess the use of capacitance as an effective radius.

By contrast, MHKC predict an effective radius proportional to the ratio of the projected area of the particle A to its maximum dimension:

$$R = \frac{C_0 \delta_0^2}{24} \times \frac{2A}{\pi D} \quad (2)$$

in the small Re limit, where C_0 , δ_0 are dimensionless parameters. For liquid drops the parameters suggested by Abraham are used ($C_0 = 0.292$, $\delta_0 = 9.06$) which matches the Stokes formula for a spherical particle (substituting $A = \pi R^2$, $D = 2R$). For ice particles, MHKC prefer $C_0 = 0.6$, $\delta_0 = 5.83$, giving a fall velocity $\sim 15\%$ higher than the Stokes result for a spherical particle[†]. We note that (2) is much more sensitive to the crystal shape than C which typically only varies by a factor of two relative to the maximum dimension of the crystal.

2.1 Planar crystals

Planar ice crystals grow at temperatures between approximately -10°C and -20°C (Pruppacher and Klett 1997). In addition to simple hexagonal plate crystals, branched and dendritic crystals may also form, particularly at high supersaturations.

For planar particles settling horizontally, Roscoe (1949) provides an analysis of the flow system, showing that it may essentially be reduced to a solution of Laplace’s equation with a constant potential on the particle surface. This is directly analogous to the problem of a stationary ice crystal growing by vapour diffusion (Pruppacher and Klett 1997, Westbrook *et al.* 2008) or the electrical potential around an earthed conducting plate of the same shape. His result for the drag is remarkably simple:

$$R = \frac{4}{3} \times C. \quad (3)$$

[†]Khvorostyanov and Curry used the smooth sphere parameters for ice particles in their 2002 study, but their subsequent paper (Khvorostyanov and Curry 2005) uses $C_0 = 0.6$, $\delta_0 = 5.83$, as do Mitchell (1996) and Mitchell and Heymsfield (2005). In this paper we will assume these latter parameters.

The derivation is straightforward, and is reproduced in appendix A. We note that in principle this result is only correct for planar particles of zero thickness; however comparison with the exact solution for an oblate spheroid suggests it is likely to be accurate for realistic crystal aspect ratios (for an aspect ratio of $L/2a = 0.1$ the difference is only 0.5%, substituting in the value of C for an oblate spheroid).

For crystals which are randomly oriented, the work of Hubbard and Douglas (1993) provides a framework to estimate the fall speed. They used an angle-averaging approximation to predict:

$$R = C \quad (4)$$

for a randomly oriented particle of arbitrary shape (not only planar particles). The essence of their approach is simply that the Oseen tensor (which acts like a Green’s function for the Navier-Stokes equations) is identical to the Green’s function for Laplace’s equation when averaged over all possible particle orientations (to within a constant factor). An overview of their theory is given in appendix B. Inserting the capacitance for a spheroid into equation 4 yields the exact Perrin (1934, 1936) formula; comparison with experimental data on non-spherical shapes yields agreement to within a few percent.

2.1.1 Hexagonal plates

The capacitance of a hexagonal plate is given by Westbrook *et al.* (2008):

$$C = 0.58a \times [1 + 0.95(L/2a)^{0.75}] \quad (5)$$

for a crystal of span ($2a$) across the basal face, and thickness L . Note plate particles correspond to $L/2a < 1$. The fall speeds of crystals with aspect ratios from 0–0.7 has been calculated using the effective radii (2), (3) and (4); these data are shown in figure 1. Also shown are experimental data from Michaeli (1977) and Kajikawa (1973)[‡] who measured the fall speeds of small ice crystals generated in a cold room. Note that to facilitate the comparison between theory and experiment the fall speeds have been normalised relative to the fall speed of a sphere with the same mass and maximum dimension (ie. relative to equation 1 with $R = D/2$). The experimental data points are in strong agreement with Roscoe’s formula (3), indicating the crystals were approximately horizontal in their orientation. Also shown are experimental data for circular discs (see Happel and Brenner 1965) falling horizontally and edge on - the fall speeds of the horizontally settling discs are within 10% of the Roscoe curve, whilst the fall speeds discs falling edge-on are slightly higher, close to the Hubbard & Douglas curve. There is similar agreement with the

[‡]Kajikawa’s data: the bin-average values from his tables 1 and 2 were used to produce the diamond data points in figures 1, 2 and 3, using the ratio of the observed fall speed to his calculated values for a circular disc/cylinder. The smallest ($20\mu\text{m}$) size bin was not plotted since Kajikawa notes that these data are inconsistent with the other size bins. This is likely a bias resulting from his use of a single power-law fit to relate crystal mass and thickness to diameter for all crystal sizes.

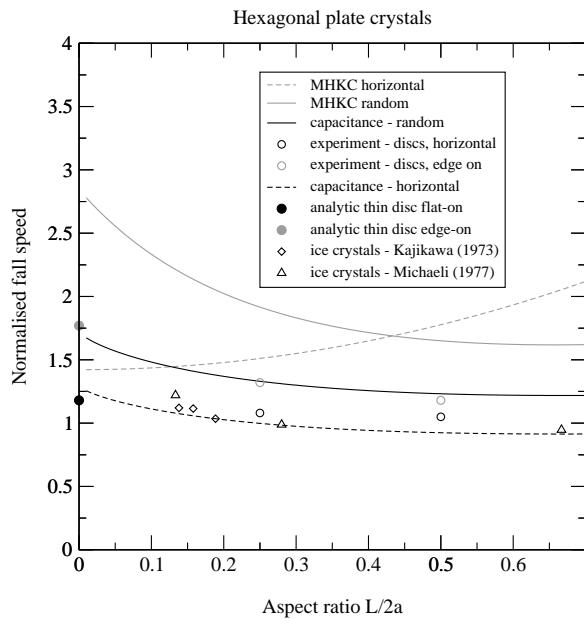


Figure 1. Fall speed of hexagonal plate ice crystals, normalised by the fall speed of a sphere with the same mass and maximum dimension. Solid black line shows Hubbard & Douglas prediction for randomly oriented crystals ($R = C$), black dashed line shows the Roscoe prediction for horizontally oriented crystals ($R = \frac{4}{3}C$). Diamonds and triangles show fall speeds of ice crystals as measured by Kajikawa (1973) and Michaeli (1977) respectively. Circles are measurements of circular discs falling horizontally (black circles) and edge-on (grey circles). Filled circles represent analytical predictions for discs of zero thickness. The MHKC predictions are shown by the grey solid line (randomly oriented) and grey dashed line (horizontally oriented).

analytic formulae for thin discs as $L/2a \rightarrow 0$ (Happel and Brenner 1965): falling flat-on the normalised velocity for a thin circular disc is 9% slower than the Roscoe estimate for a thin hexagonal plate, which seems sensible (slightly more drag on a disc than a hexagonal plate with the same radius). Edge-on, the disc falls 3% faster than the Hubbard and Douglas estimate for a thin, randomly oriented hexagonal plate.

Jayaweera and Ryan (1972) also measured the fall speed of small plate crystals; however, unlike their measurements of columnar crystals (see section 2.2) they did not explicitly record the crystal aspect ratio. Assuming an aspect ratio of $L/2a = 0.1$ their fit corresponds to a normalised fall speed of 1.45, which lies in-between the Roscoe and Hubbard & Douglas predictions.

The MHKC predictions are shown in figure 1 assuming both randomly oriented crystals ($A = a^2[1.3 + 3(L/2a)]$) and horizontally oriented crystals ($A = 2.6a$). The former assumption is recommended by Mitchell (1996) for crystals with $Re < 10$. It is apparent that both of the MHKC curves overestimate the observations. For the randomly oriented assumption the prediction is $\sim 70\%$ too high over the range of aspect ratios considered here. Applying the horizontally oriented assumption offers an improvement for thin crystals, reducing the error to 20% for an aspect ratio of 0.15. Unfortunately the errors are much worse for thick plates ($L/2a = 0.65$) where the fall

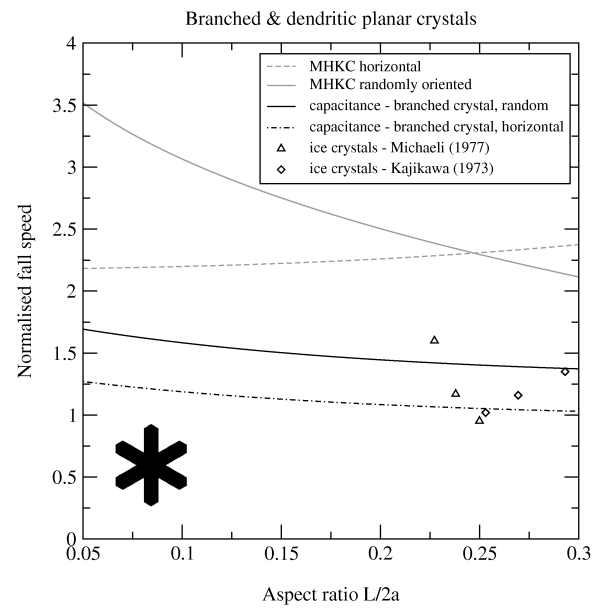


Figure 2. Fall speed of branched and dendritic planar ice crystals, normalised by the fall speed of a sphere with the same mass and maximum dimension. Solid black line shows Hubbard & Douglas prediction for randomly oriented crystals ($R = C$), black dashed line shows the Roscoe prediction for horizontally oriented crystals ($R = \frac{4}{3}C$). Diamonds and triangles show fall speeds of ice crystals as measured by Kajikawa (1973) and Michaeli (1977) respectively. The MHKC predictions are shown by the grey solid line (randomly oriented) and grey dashed line (horizontally oriented). Inset is the branched crystal model used in the capacitance and projected area calculations.

speed is now overestimated by more than a factor of 2. The strong sensitivity of equation 2 to crystal orientation appears to be unphysical given the relatively weak dependence on fall attitude observed for circular discs (for very thin discs edge-on is 50% faster than the flat-on).

2.1.2 Branched & dendritic crystals

Kajikawa (1973) and Michaeli (1977) also made measurements of the fall speed of branched and dendritic crystals, and their experimental results are shown in figure 2. Based on photographs in Kajikawa's paper the capacitance of a 'representative' branched crystal has been calculated for aspect ratios between $L/2a = 0.05$ – 0.3 using the method outlined in Westbrook *et al.* (2008). The outline of the model crystal is shown inset in figure 2. The width of the branches is 35% of their length from the crystal centre. The overall span from tip to tip across the crystal is defined as $(2a)$ and the thickness as L in the same way as for the hexagonal plate crystals. The values of C were only marginally lower than for a solid hexagonal plate (by approximately 5–10%). The capacitance data were substituted into equations 3 and 4, and curves fitted to the resulting fall speed predictions: these are shown in figure 2.

The experimental data appear to be in broad agreement with the Roscoe and Hubbard & Douglas theories, with most of the points lying between the two curves. The

scatter is wider than for the hexagonal plate data, perhaps indicating a broader distribution of crystal orientations; however we also note that the aspect ratio recorded by Michaeli (unlike for his hexagonal plate and column crystals) was not directly measured, but assumed from the relationship given by Auer and Veal (1970), and this is likely to introduce some error into the comparison. In addition we may expect the capacitance of the observed crystals to vary by around $\pm 10\%$.

Also shown in figure 2 is the MHKC predictions for the model crystal described above. Assuming either horizontal or randomly oriented crystals, it is found that the MHKC formula overestimates the observed crystal fall speeds by $\sim 80\%$ for an aspect ratio of 0.25 (where most of the experimental data is clustered). This is particularly an issue for crystals with thin branches and dendritic features where the projected area A is very small but the capacitance is only marginally reduced relative to a solid hexagonal plate (typically by only $\sim 25\%$, see Westbrook *et al.* 2008). If the capacitance is the appropriate length scale then this implies that MHKC theory will increasingly overestimate the crystal fall speed as the crystals become more tenuous.

2.2 Columnar ice crystals

Hexagonal column crystals grow at temperatures colder than -20°C and also in a window between -5 and -10°C (Pruppacher and Klett 1997). Jayaweera and Ryan (1972) made direct measurements of crystal mass, length, width and fall speed, and these are plotted in figure 3. Similar measurements were made by Kajikawa (1973) and Michaeli (1977), also shown in figure 3.

The capacitance of a hexagonal column of length L and width $(2a)$ is given by equation 5 with $L/2a > 1$. Substituting this into the Hubbard and Douglas formula (4) yields the black line plotted in figure 3. Although there is significant scatter in the experimental data, the bulk of the observations are in agreement with the Hubbard & Douglas curve to within $\sim 20\%$. The agreement with experimental data for circular cylinders falling horizontally and end-on (see Happel and Brenner 1965) is also good, to within $\sim 10\%$. The cylinders falling end-on have a slightly higher fall speed than the Hubbard & Douglas curve (4), whilst cylinders falling horizontally have a slightly lower fall speed than (4), which seems sensible since the Hubbard-Douglas theory is intended to represent the average over all orientations.

Also shown in figure 3 is the MHKC prediction for randomly and horizontally oriented columns. As for planar crystals, both MHKC curves strongly overestimate the experimental data, by around 50% for an aspect ratio of 1.5, and by more than a factor of two for aspect ratios $L/2a > 3$. Neither MHKC curve is consistent with the data for circular cylinders.

2.3 Polycrystals

Bullet-rosettes are often the dominant crystal habit in cirrus clouds (Heymsfield and Iaquinta 2000) which are

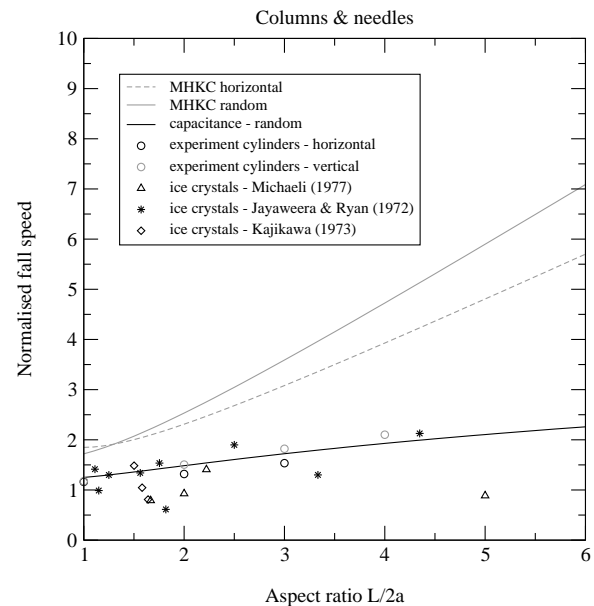


Figure 3. Fall speed of hexagonal column and needle ice crystals, normalised by the fall speed of a sphere with the same mass and maximum dimension. Solid black line shows Hubbard & Douglas prediction for randomly oriented crystals ($R = C$). Stars, diamonds and triangles show fall speeds of ice crystals as measured by Jayaweera and Ryan (1972), Kajikawa (1973) and Michaeli (1977) respectively. Circles are measurements of circular cylinders falling horizontally (black circles) and end-on (grey circles). The MHKC predictions are shown by the grey solid line (randomly oriented) and grey dashed line (horizontally oriented).

typically composed of between two and six bullet crystals in a radial formation. Small ‘embryonic’ bullet-rosettes less than $100\mu\text{m}$ in diameter have been observed (see figure 2 of Heymsfield and Iaquinta), and the fall speeds of these particles have been estimated using the Hubbard & Douglas and MHKC theories. There are (to the author’s knowledge) no direct observations of the sedimentation velocity of these tiny rosettes.

The capacitance of various bullet-rosettes models has been calculated by Westbrook *et al.* (2008), who derived the fit $C = 0.40D \times (L/2a)^{-0.25}$ for rosettes with six arms. Here L is the length of the columnar section of the bullets, and $(2a)$ is their width. The pyramid ends were assumed to be $(L/2)$ in length. Using this data, the fall speeds of bullet-rosettes with a variety of aspect ratios has been calculated using equation 4, as shown in figure 4.

Also shown in figure 4 are the fall speeds of the same model crystals using the MHKC method. As above, random orientation is assumed. At aspect ratios close to unity the MHKC fall speeds are $\sim 40\%$ higher than the capacitance predictions, whilst for rosettes with thin arms $L/2a = 4$ the fall speeds are a factor of 3 larger than the Hubbard & Douglas prediction. This implies that the MHKC formula may be grossly overestimating the sedimentation rate of small rosette crystals, especially those with thin arms.

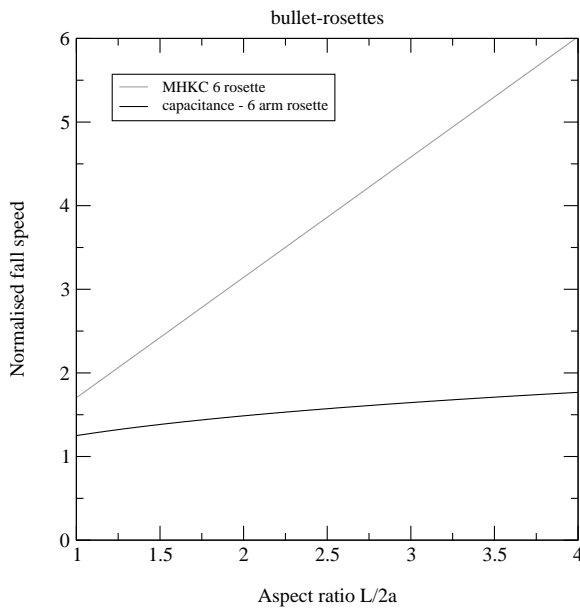


Figure 4. Fall speed of randomly-oriented bullet-rosette ice crystals, normalised by the fall speed of a sphere with the same mass and maximum dimension. Black line shows Hubbard & Douglas prediction for rosettes with six branches; grey line shows corresponding MHKC prediction.

3 Discussion

The sedimentation rate of small ice crystals with maximum dimension less than $\sim 100\mu\text{m}$ have been estimated by exploiting analogies with electrostatics and molecular-diffusion problems. The capacitance of the particles was found to be an appropriate length scale to characterise the crystal drag: for planar crystals settling horizontally $R = \frac{4}{3}C$ is suggested, for other types $R = C$. These predictions compare well with experimental data for hexagonal plates, branched and dendritic crystals and columns. The method has also been applied to bullet-rosettes. The results are in substantial conflict with MHKC's predicted fall speeds, which grossly overestimate the sedimentation rates of these tiny crystals, due to their characteristic length scale being over-sensitive to crystal shape and orientation. Capacitance is a much less sensitive parameter, varying between $C/D \simeq 0.2$ for thin-armed rosettes and needle crystals to $C/D \simeq 0.4$ for short columns with aspect ratio close to unity.

From a physical point of view it is perhaps unsurprising that the MHKC boundary-layer formulation fails for $\text{Re} \ll 1$. However the suggestion from Mitchell (1996) and Khvorostyanov and Curry (2005) was that equation 2 would hold, largely based on the fact that the comparison with Stokes equation for a spherical particle is so good (see section 2); unfortunately the comparisons with experimental data in this paper show that it does not hold in general for non-spherical ice crystals. Interestingly, Mitchell (1996) did make a comparison with the experiment of Yagi (1970) who measured the average fall speed of an ice fog composed of crystals with a mean size close to $100\mu\text{m}$ and found $\langle v \rangle = 0.107 \text{ ms}^{-1}$. Mitchell used the recorded mean diameter for each habit, and used mass-

and area-diameter relationships derived from other studies to estimate $\langle v \rangle = 0.097 \text{ ms}^{-1}$, in apparent agreement. However because the crystals were distributed in size and the mass/area/size relationships had to be assumed, the comparison is rather uncertain, particularly since the relationship between crystal size and velocity is non-linear. The comparisons made in this paper with the direct measurements of individual crystals by Jayaweera and Ryan (1972), Kajikawa (1973) and Michaeli (1977) are a much stronger test of the MHKC formula, and one which appears much less favourable to it at small Reynolds number.

The fall speeds of these tiny crystals are of interest for the interpretation of Doppler lidar measurements in cirrus. It should be possible to assess the dominance of crystals smaller than $60\mu\text{m}$ on the optical properties of cirrus cloud by examining the frequency distribution of measured Doppler lidar velocities in such clouds. Using the results from section 2 we find that the maximum fall speed for a $D = 60\mu\text{m}$ crystal is 0.07 ms^{-1} : this value corresponds to a compact hexagonal column with an aspect ratio of one, and a density equal to that of solid ice. The temperature was assumed to be -60°C ; at -10°C the maximum fall velocity is reduced to 0.06 ms^{-1} . Note that the fall speed measurements by Jayaweera and Ryan (1972), Kajikawa (1973) and Michaeli (1977) included crystals over $100\mu\text{m}$ in size, and none of them fell faster than 0.06 ms^{-1} . If the lidar backscatter is dominated by these tiny slow-sedimenting crystals, then the measured mean Doppler velocity should also be dominated by them since it is weighted by the backscatter. Analysis of 1 year of continuous measurements from a $1.5\mu\text{m}$ vertically-pointing Doppler lidar at the Chilbolton Facility for Atmospheric and Radio Research in Hampshire is in progress, and the results should help to inform the small ice debate.

The results presented here may also be of interest to modellers studying the effect that large concentrations of small crystals have on GCM results (Mitchell *et al.* 2006), as well as for researchers modelling the advection and persistence of contrails (Duda *et al.* 2004).

For $\text{Re} > 1$ the drag becomes increasingly determined by A and the MHKC relationship has proved rather successful at accurately predicting ice particle fall speeds, offering good agreement with experimental data for most particle types. Some interesting discrepancies remain however: consider a Doppler measurement of a solid ice needle crystal, aspect ratio = 10, observed falling at 0.40 ms^{-1} . The retrieved crystal size would be $D = 600 \mu\text{m}$ assuming MHKC; compare that to $D = 1 \text{ mm}$ assuming Jayaweera and Cottis's (1969) relationship for circular cylinders. This constitutes a substantial error bar on the retrieved crystal size. Doppler measurements are increasingly forming an integral part of radar retrieval algorithms (eg. Delanoë *et al.* 2007) and it is important therefore that these kinds of discrepancies be resolved. By contrast the MHKC prediction for a short column with $L/2a = 2$ are in excellent agreement Jayaweera and Cottis's cylinder data for the same range of crystal sizes. More

extensive testing would be valuable to assess the universality of the MHKC formula, although the practicalities of simultaneous estimates of crystal fall speed, mass, area and maximum dimension make direct comparisons challenging.

Finally the author notes that the theoretical approach applied in this work (in particular that of Hubbard and Douglas 1993) is likely to be applicable to non-spherical aerosol particles, allowing accurate estimates of the sedimentation rate and mobility of complex, irregular aerosols to be made. The only caveat is that the Hubbard and Douglas derivation assumes ‘stick’ boundary conditions, and so may not be suitable for sub-micron particles without an appropriate slip correction.

4 Appendix A: horizontally oriented planar crystals

Here the drag on a thin ($L \ll 2a$) planar crystal settling horizontally with velocity u_0 is derived, following Roscoe (1949). The Stokes equations are:

$$\eta \nabla^2 u = \frac{\partial p}{\partial x}, \eta \nabla^2 v = \frac{\partial p}{\partial y}, \eta \nabla^2 w = \frac{\partial p}{\partial z} \quad (6)$$

where the velocity components u, v, w (corresponding to the x, y, z axes) satisfy the continuity equation:

$$\frac{\partial u}{\partial x} + \frac{\partial v}{\partial y} + \frac{\partial w}{\partial z} = 0. \quad (7)$$

and for convenience we assume $u = v = w = 0$ on the crystal surface, and $u = u_0, v = 0, w = 0$ far from the crystal. The x direction is taken as the vertical axis.

A flow system which satisfies (7) is:

$$u = \phi - x \frac{\partial \phi}{\partial x}, v = -x \frac{\partial \phi}{\partial y}, w = -x \frac{\partial \phi}{\partial z} \quad (8)$$

if $\nabla^2 \phi = 0$ (ie. if ϕ is a solution of Laplace’s equation). Substituting this into equation 6 the velocities (8) satisfy the Stokes equations provided that:

$$p = -2\eta \frac{\partial \phi}{\partial x}. \quad (9)$$

Consider then an earthed conductor with the same shape as the crystal. Taking $\phi = 0$ on the surface of the crystal and $\phi = u_0$ far from the crystal matches the boundary conditions on u, v, w , and we identify (8) as the flow system round the ice crystal with ϕ the electrical potential around the analogous conductor.

The normal stress on the surface of the crystal is equal to p . The net force normal to the plate is therefore the difference between p on either side of the crystal, ie. $\delta p = 2\eta \times 4\pi\sigma$ per unit area of surface (applying Gauss’s law), where σ is the charge density on the conductor. Integrating σ over the whole surface leads to the total translational drag force on the crystal, ie:

$$\text{Drag} = 8\pi\eta u_0 C \quad (10)$$

since the total charge on the conductor is simply the capacitance C multiplied by the applied voltage u_0 . Comparing this result with Stokes law (1) leads to the conclusion:

$$R = \frac{4}{3}C \quad (11)$$

for planar ice crystals which are sufficiently thin relative to the dimensions of their horizontal cross-section.

5 Appendix B: randomly oriented crystals

Here the average drag on a randomly oriented ice crystal is estimated using the approach of Hubbard and Douglas (1993). Consider the Oseen tensor, which describes a point hydrodynamic source (Happel and Brenner 1965):

$$\mathbf{T}(\mathbf{R}) = \frac{1}{8\pi\eta R} \left(\mathbf{I} + \frac{\mathbf{R}\mathbf{R}}{R^2} \right) \quad (12)$$

where \mathbf{I} is the identity matrix, and $\mathbf{R} = \mathbf{r}' - \mathbf{r}$. The orientational average of \mathbf{T} is given by:

$$T = \frac{1}{6\pi\eta R} \quad (13)$$

where $R = |\mathbf{R}|$, ie. T is identical to the Green’s function for Laplace’s equation $(4\pi R)^{-1}$ to within a constant factor. Based on this observation, consider the average flux of momentum away from the ice crystal:

$$\int \sigma T ds = \frac{1}{6\pi\eta} \times \phi(\mathbf{r}) \quad (14)$$

where ds is a small element of surface area, and we define σ to be the momentum flux density. Given the above considerations the scalar function $\phi(\mathbf{r})$ must satisfy Laplace’s equation, and σ may analogously be interpreted as the density of charge on the surface of a conductor with the same size and shape as the ice crystal.

The stress tensor \mathbf{S} is constructed so as to conserve linear and angular momentum, and to ensure that \mathbf{u}_0 and the associated drag are co-linear:

$$\mathbf{S} = 6\pi\eta [(\nabla\phi)\mathbf{u}_0 + \mathbf{u}_0(\nabla\phi) - (\nabla\phi) \cdot (\mathbf{u}_0)\mathbf{I}] \quad (15)$$

where $\phi = 1$ on the surface of the particle, and $\phi = 0$ in the far-field. Then the Stokes equations are:

$$\nabla \cdot \mathbf{S} = 6\pi\eta \mathbf{u}_0 \nabla^2 \phi = 0. \quad (16)$$

Essentially then, the flow system is described purely in terms of the electrical potential ϕ around a conductor of the same size and shape as the ice crystal. The angle-averaged fluid velocity at a given point is $\mathbf{u}(\mathbf{r}) = \mathbf{u}_0 \phi(\mathbf{r})$.

Given the stress components above, the drag force on the particle is:

$$\left| 6\pi\eta \int \mathbf{S} \cdot \mathbf{n} ds \right| \quad (17)$$

where \mathbf{n} is the unit vector pointing normal to the crystal surface (outwards into the fluid). Using the analogy developed above, the gradient $\nabla\phi$ may be interpreted in terms

of the electrical potential gradient near a conductor of the same shape and size as the particle, ie $(\nabla\phi)_{\text{surface}} = -\sigma\mathbf{n}$. The total drag force is then simply:

$$\text{Drag} = 6\pi\eta|\mathbf{u}_0|C \quad (18)$$

ie. Stokes formula (1) with $R = C$.

Acknowledgements

Helpful discussions with Jack Douglas (NIST, USA) are gratefully acknowledged. This work was supported by the Natural and Environmental Research Council.

References

- Abraham FF 1970. Functional dependence of drag co-efficient of a sphere on Reynolds number. *Phys. Fluid.* **13**: 2194-2195
- Böhm HP 1989. A general equation for the terminal fall speed of solid hydrometeors. *J. Atmos. Sci.* **46**: 2419-2427
- Delanoë J, Protat A, Bouniol D, Heymsfield A, Bansemmer A, Brown P 2007. The characterization of ice cloud properties from Doppler radar measurements. *J. Appl. Met. & Clim.* **46**: 1682-1698
- Field PR, Wood R, Brown PRA, Kaye PH, Hirst E, Greenaway R, Smith JA 2003. Ice particle interarrival times measured with a fast FSSP. *J. Atmos. & Ocean. Tech.* **20**: 249-261
- Happel J, Brenner H. 1965. *Low Reynolds number hydrodynamics*. Prentice-Hall.
- Heymsfield AJ and Iaquinta J 2000. Cirrus crystal terminal velocities. *J. Atmos. Sci.* **57**: 916-938
- Heymsfield AJ, Lewis S, Bansemmer A, Iaquinta J, Miloshevich LM, Kajikawa M, Twohey C, Poellot MR 2002. A general approach for deriving the properties of cirrus and stratiform ice cloud particles. *J. Atmos. Sci.* **59**: 3-29
- Hubbard JB and Douglas JF 1993. Hydrodynamic friction of arbitrarily shaped Brownian particle. *Phys. Rev. E* **47**: R2983-2986
- Jayaweera KOLF and Cottis BF 1969. Fall velocities of plate-like and columnar ice crystals. *Q. J. Roy. Meteor. Soc.* **95**: 703-709
- Jayaweera KOLF and Ryan BF 1972. Terminal velocities of ice crystals. *Q. J. Roy. Meteor. Soc.* **98**: 193-197
- Kajikawa M 1973. Laboratory measurements of falling velocity of individual ice crystals. *J. Meteor. Soc. Japan* **51**: 263-272
- Khvorostyanov VI and Curry JA 2002. Terminal velocities of droplets and crystals: power laws with continuous parameters over the size spectrum. *J. Atmos. Sci.* **59**: 1872-1884
- Khvorostyanov VI and Curry JA 2005. Fall velocities of hydrometeors in the atmosphere: refinements to a continuous analytical power law. *J. Atmos. Sci.* **62**: 4343-4357
- McFarquhar GM, Um J, Freer M, Baumgardner D, Kok GL and Mace G 2007. Importance of small ice crystals to cirrus properties: observations from the Tropical Warm Pool International Cloud Experiment (TWP-ICE). *Geophys. Res. Lett.* **34**: L13803
- Mitchaeli G 1977. Settling velocities of small ice crystals. *Tellus* **29**: 282-285
- Mitchell DL 1996. Use of mass- and area-dimensional power laws for determining precipitation particle terminal velocities. *J. Atmos. Sci.* **53**: 1710-1723
- Mitchell DL and Heymsfield AJ 2005. Refinements in the treatment of ice particle terminal velocities, highlighting aggregates. *J. Atmos. Sci.* **62**: 1637-1644
- Mitchell DL, Rasch P, Ivanova D, McFarquhar G and Nousianen T 2006. The impact of controversial small ice crystals on GCM simulations. 12th AMS conference on cloud physics, Madison, USA, preprint: <http://ams.confex.com/ams/pdfpapers/113642.pdf>
- Perrin E 1934. Dispersion diélectrique pour des molécules ellipsoïdales. *J. Phys. Radium* **5**: 497
- Perrin E 1936. Mouvement Brownian d'un ellipsoïde (II). Rotation libre et dépolarisation des fluorescences. Translation et diffusion des molécules ellipsoïdales. *J. Phys. Radium* **7**: 1
- Pruppacher HR, Klett JD. 1997. *Microphysics of clouds and precipitation* (2nd edn). Kluwer.
- Roscoe R 1949. The flow of viscous fluids round plane obstacles. *Philos. Mag.* **40**: 338-351
- Westbrook CD, Hogan RJ and Illingworth AJ 2008. The capacitance of pristine ice crystals and aggregate snowflakes. *J. Atmos. Sci.* in press, preprint available <http://arxiv.org/pdf/physics/0610038>
- Yagi T 1970. Measurement of the fall velocity of ice crystals drifting in a supercooled fog. *J. Meteor. Soc. Japan* **48**: 287-292